

Naval Research Laboratory

Washington, DC 20375-5000



AD-A240 680



NRL Memorandum Report 6887

Tilted Resonator Experiments on A Quasioptical Gyrotron

T. A. HARGREAVES, A. W. FLIFLET, R. P. FISCHER, M. L. BARSANTI,*
W. M. MANHEIMER, B. LEVUSH,** AND T. M. ANTONSEN, JR***†

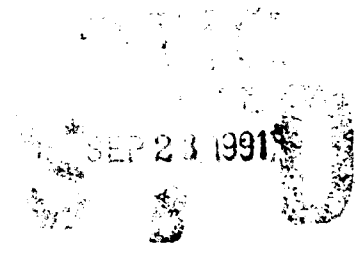
*Beam Physics Branch
Plasma Physics Division*

**B-K Systems, Inc.,
Rockville, MD 20850*

***Laboratory for Plasma Research
University of Maryland,
College Park, MD 20742*

****Science Applications International Corp.
McLean, VA 22102*

September 16, 1991



91-11220



REPORT DOCUMENTATION PAGE			Form Approved OMB No. 0704-0188	
Public reporting burden for this collection of information is estimated to average 1 hour per response, including the time for reviewing instructions, searching existing data sources, gathering and maintaining the data needed, and completing and reviewing the collection of information. Send comments regarding this burden estimate or any other aspect of this collection of information, including suggestions for reducing this burden, to Washington Headquarters Services, Directorate for Information Operations and Reports, 1215 Jefferson Davis Highway, Suite 1204, Arlington, VA 22202-4302, and to the Office of Management and Budget, Paperwork Reduction Project (0704-0188), Washington, DC 20503				
1. AGENCY USE ONLY (Leave blank)	2. REPORT DATE 1991 September 16	3. REPORT TYPE AND DATES COVERED		
4. TITLE AND SUBTITLE Tilted Resonator Experiments on a Quasioptical Gyrotron			5. FUNDING NUMBERS	
6. AUTHOR(S) T. A. Hargreaves, A. W. Fliflet, R. P. Fischer, M. L. Barsanti,* W. M. Manheimer, B. Levush,** and T. M. Antonsen, Jr.**†				
7. PERFORMING ORGANIZATION NAME(S) AND ADDRESS(ES) Naval Research Laboratory Washington, DC 20375-5000			8. PERFORMING ORGANIZATION REPORT NUMBER NRL Memorandum Report 6887	
9. SPONSORING / MONITORING AGENCY NAME(S) AND ADDRESS(ES) U. S. Department of Energy Washington, DC 20545			10. SPONSORING / MONITORING AGENCY REPORT NUMBER Office of Naval Research Arlington, VA 22217	
11. SUPPLEMENTARY NOTES *B-K Systems, Inc., Rockville, MD 20850 **Laboratory for Plasma Research, University of Maryland, College Park, MD 20742 **†Science Applications International Corp., McLean, VA 22102				
12a. DISTRIBUTION / AVAILABILITY STATEMENT Approved for public release; distribution unlimited.			12b. DISTRIBUTION CODE	
13. ABSTRACT (Maximum 200 words) Tilting the resonator axis slightly with respect to the magnetic field axis in the quasioptical gyrotron (QOG) is predicted to greatly enlarge the parameter space available for stable, single-mode operation. Greater interaction efficiency is also predicted for single-mode operation. A resonator with a 2° tilt has been tested on the QOG experiment at the Naval Research Laboratory (NRL). The operation of this resonator has been compared to an untilted, but otherwise identical resonator. Multimode operation of the two resonators was very similar, in contrast to predictions. However, an output power of 600 kW was produced at an efficiency of 8% and a frequency of 120 GHz. At lower power, efficiencies above 12% were observed. The efficiency of single-mode operation appears to be raised significantly by tilting the resonator axis.				
14. SUBJECT TERMS Quasioptical QOG Gyrotron			15. NUMBER OF PAGES 28	
			16. PRICE CODE	
17. SECURITY CLASSIFICATION OF REPORT UNCLASSIFIED	18. SECURITY CLASSIFICATION OF THIS PAGE UNCLASSIFIED	19. SECURITY CLASSIFICATION OF ABSTRACT UNCLASSIFIED	20. LIMITATION OF ABSTRACT SAR	

I. INTRODUCTION	1
II. SINGLE-MODE RESULTS	2
III. NUMERICAL RESULTS	8
IV. DESCRIPTION OF EXPERIMENT	10
V. EXPERIMENTAL RESULTS	14
VI. DISCUSSION	17
VII. CONCLUSIONS	21
ACKNOWLEDGEMENTS	22
REFERENCES	23



Accession For	
NTIS GRA&I	<input checked="" type="checkbox"/>
DTIC TAB	<input type="checkbox"/>
Unannounced	<input type="checkbox"/>
Justification	
by	
DTIC TAB	
Availability Codes	
Avail and/or	
Special	
Dist	Special
A-1	

TILTED RESONATOR EXPERIMENTS ON A QUASIOPTICAL GYROTRON

I. INTRODUCTION

There is currently a need for megawatt average power sources in the 100–300 GHz range for electron cyclotron heating (ECH) of fusion plasmas. For example, the Compact Ignition Tokamak (CIT) design¹ includes 30 MW of 280 GHz radiation and the International Thermonuclear Experimental Reactor (ITER) design² requires 20 MW of 140 GHz rf power. The leading candidate for such a source is the waveguide cavity gyrotron,³ having produced an output power of 940 kW at an efficiency of 35% and a frequency of 140 GHz,⁴ and 1.2 MW at an efficiency of 20% at 148 GHz⁵ in a continuous-wave (CW) relevant configuration. However, as the frequency and power are increased, these gyrotrons are forced to use more highly overmoded cavities, larger collectors, and vacuum output windows capable of handling the higher powers. The quasioptical gyrotron⁶ (QOG) is a reasonable alternative to the cavity gyrotrons that offers several advantages. The QOG resonator is made up of a pair of spherical mirrors of small diameter, effectively eliminating all but the lowest order transverse mode via large diffraction losses. The mirror separation can be relatively large, reducing the ohmic heating density on the mirrors far below that of current continuous-wave (cw) gyrotrons and creating a large interaction volume allowing the use of a high-current, low current-density electron beam. This configuration also implies that there exist several longitudinal modes within the interaction bandwidth of the device, making multimode operation possible. Multimode operation has been studied both theoretically and numerically⁷ as well as experimentally.⁸ In the QOG the radiation and the electron beam propagate perpendicular to each other, allowing complete freedom in the design of the collector. Implementation of a depressed collector for energy recovery of the spent electron beam is easily accomplished.⁹ Frequency tunability may be accomplished by varying either the electron beam energy or the magnetic field while maintaining the same output mode.¹⁰ A gaussian mode may be coupled out of the resonator directly by replacing one of the resonator mirrors by an appropriately designed diffraction grating placed in the Littrow mount position.¹¹

One problem common to all QOG experiments performed to date is the relatively low efficiency, particularly for single-moded operation. This is due in part to the fact that some of the electrons in an annular beam pass through the resonator on electric field nulls of the standing wave pattern. These electrons and those passing through the resonator at low electric fields do not interact efficiently with the resonator fields, causing the total interaction efficiency to be degraded by approximately 1/3 compared to the case of a pencil beam, where all electrons pass through the resonator on a peak of the standing wave.¹² Another consequence of the variation in electron coupling is the reduction in the stable single-mode operating region. One approach to alleviating this problem is to tilt the resonator axis slightly with respect to the plane perpendicular to the direction of electron beam propagation. The tilt should be enough to ensure that all electrons in the beam pass through at least one peak of the standing wave, and is predicted to both enhance the interaction efficiency and to greatly increase the parameter range of stable, single-mode operation.¹³ This approach has been tested experimentally and is the subject of this paper.

The remainder of the paper is organized as follows. The theory which motivates the experiment is described in Section II with multimode numerical results presented in Sec-

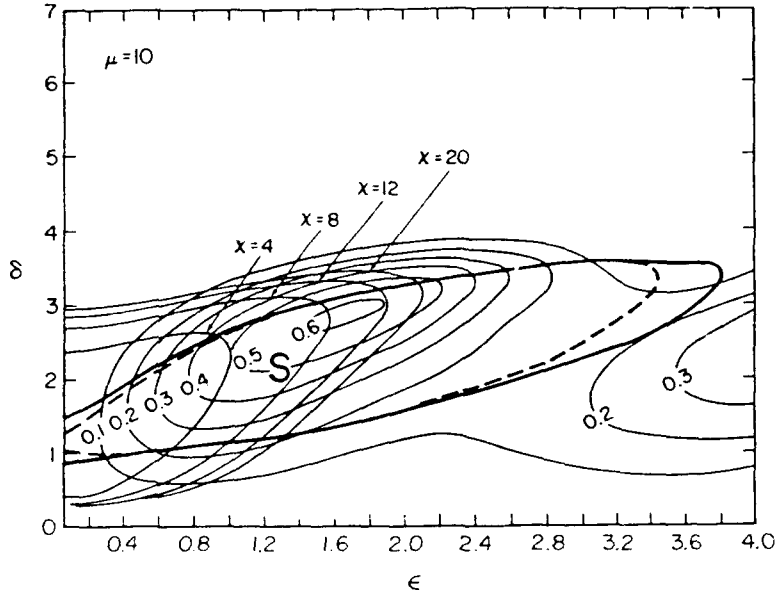


Figure 1: Stability boundary for single-mode operation with a pencil electron beam with $\mu = 10$. The solid and dotted lines correspond to $T_0 = 10$ and 50 , respectively.

tion III. The experimental setup is given in Section IV and the results are reported in Section V. Section VI includes a discussion of the results as well as a comparison to theory, with some conclusions presented in Section VII.

II. SINGLE-MODE RESULTS

The extension of the single-mode equations of motion to include a small tilt angle have been described in detail elsewhere.¹³ Single-mode operation is desirable for many applications, but is not guaranteed due to the large number of resonator modes within the interaction bandwidth of the QOG. Therefore, it is important to study the stability of the QOG resonator operating in a single mode. This too has been done,¹³ and the results of the analysis are presented here. The region of stable, single-mode operation is shown in Fig. 1 as the area labeled S within the solid curve. This calculation is for a pencil electron beam and an untilted resonator. Level curves of perpendicular efficiency (η_{\perp}) are plotted and reach 60%, where the total efficiency is related to the perpendicular efficiency via

$$\eta = \left[\beta_{\perp}^2 / 2 (1 - \gamma^{-1}) \right] \eta_{\perp} \quad (1)$$

where β_{\perp} is the electron velocity perpendicular to the magnetic field divided by the velocity of light and γ is the electron relativistic factor prior to the interaction. Also plotted in the figure are curves of constant normalized current $\chi = I/I_{st}$ where I is the electron beam current, I_{st} is the minimum threshold current, minimized over all values of magnetic field detuning δ . The normalized magnetic field detuning, electric field (ϵ) and interaction length

(μ) are defined as

$$\delta = (\omega - \Omega / \gamma) w_o / v_z = \frac{\mu \Delta}{2} \quad (2)$$

$$\epsilon = \frac{2\pi}{c\beta_{\perp}\beta_{\parallel}} \frac{E w_o}{B \lambda} = F \mu \quad (3)$$

$$\mu = 2\pi \frac{\beta_{\perp}^2 w_o}{\beta_{\parallel} \lambda} \quad (4)$$

where ω is the angular frequency of the radiation, Ω is the nonrelativistic electron cyclotron frequency, w_o is the radiation waist radius, v_z is the electrons velocity parallel to the applied magnetic field, $\beta_{\parallel} = v_z/c$, c is the velocity of light, F is the peak electric field in the resonator, B is the applied magnetic field strength, λ is the wavelength of the radiation, and F and Δ are the normalized electric field and detuning parameters defined in the literature.¹⁴ The solid and dashed stability boundaries in Fig. 1 correspond to different values of the normalized spectral width (T_o^{-1}) of the resonator where $T_o = 2dv_z / (w_o c)$ and d is the resonator mirror separation.

An annular electron beam rather than a pencil beam was used in the experiments described here due to its availability and high-power capability. Unfortunately, the region of stable, single-mode operation decreases dramatically when an annular electron beam is used in place of the pencil beam, as can be seen in Fig. 2. The reason for this is that when the pencil beam is placed on the electric field peak of a given mode, the beam then couples equally to all modes having the same parity. Further, it does not couple at all to modes of the opposite parity. Since the beam couples equally well to the dominant mode and each of the modes that needs to be suppressed, the suppression by the dominant mode can be very effective. This is no longer the case when an annular electron beam having a diameter greater than $\lambda/2$ is used. Now the electrons that are on the electric field peak of the desired mode interact as in a pencil beam, but there are also electrons passing through the resonator on the null of the standing wave pattern of the desired mode and do not interact with it. However, these electrons are located on the electric field peak of the modes of opposite parity and are free to interact strongly with those modes. This is the reason that it is more difficult for the desired mode to suppress the growth of undesired modes when an annular electron beam is used. From Fig. 2 it is also evident that the use of an annular beam implies that the parameters for optimum efficiency operation lie outside the region of stable single-mode operation. It should be noted that the efficiencies shown in these figures were calculated assuming a single mode in the resonator and are not strictly valid outside the single-mode stability region. Outside this region the effects of multiple modes in the resonator should be included.

The size of the stability region may be increased by simply tilting the resonator axis by a small angle (θ) with respect to the plane perpendicular to the magnetic field. This effect is demonstrated in Fig. 3 where the normalized resonator tilt angle is $\theta' = kw_o\theta$ and $k = 2\pi/\lambda$ is the wave number of the radiation. As can be seen, the peak efficiency is again inside the stable, single-mode operating region and perpendicular efficiencies in excess of 50% are predicted. Insight into the effectiveness of such a small tilt angle can be gained

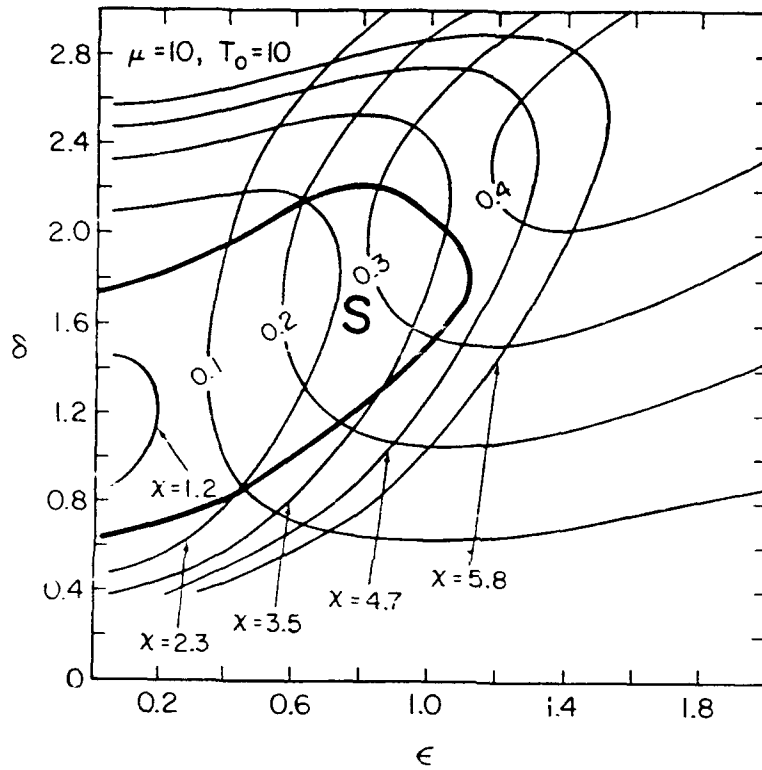


Figure 2: Stability boundary for single-mode operation with an annular electron beam ($kr_0 = 4.0$, r_0 is the beam radius) with $\mu = 10$ and $T_0 = 10$.

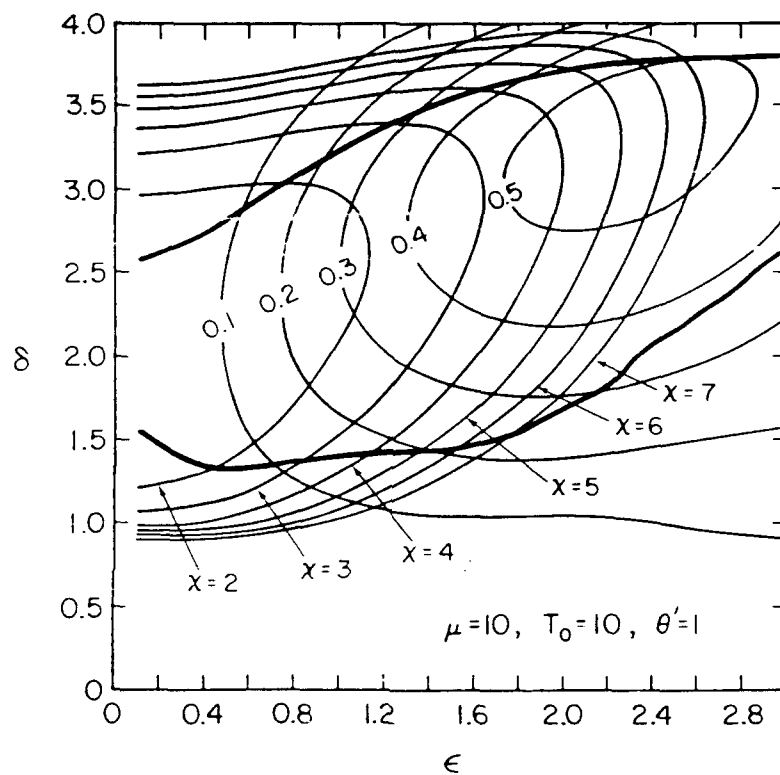


Figure 3: Stability boundary for single-mode operation with an annular electron beam ($kr_0 = 4.0$) in a tilted resonator with $\mu = 10$, $\theta' = 1.0$ and $T_0 = 10$.

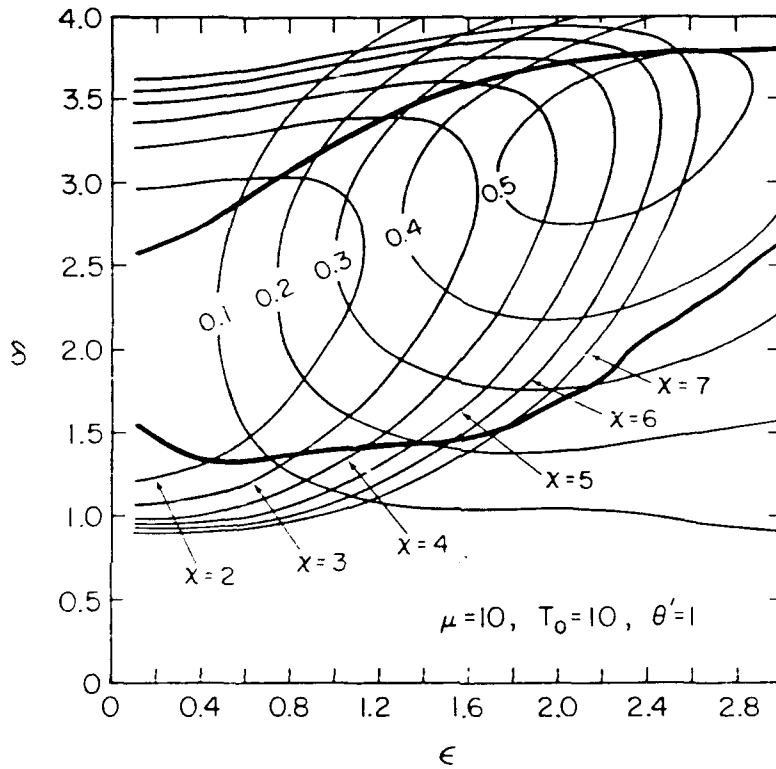


Figure 3: Stability boundary for single-mode operation with an annular electron beam ($kr_0 = 4.0$) in a tilted resonator with $\mu = 10$, $\theta' = 1.0$ and $T_0 = 10$.

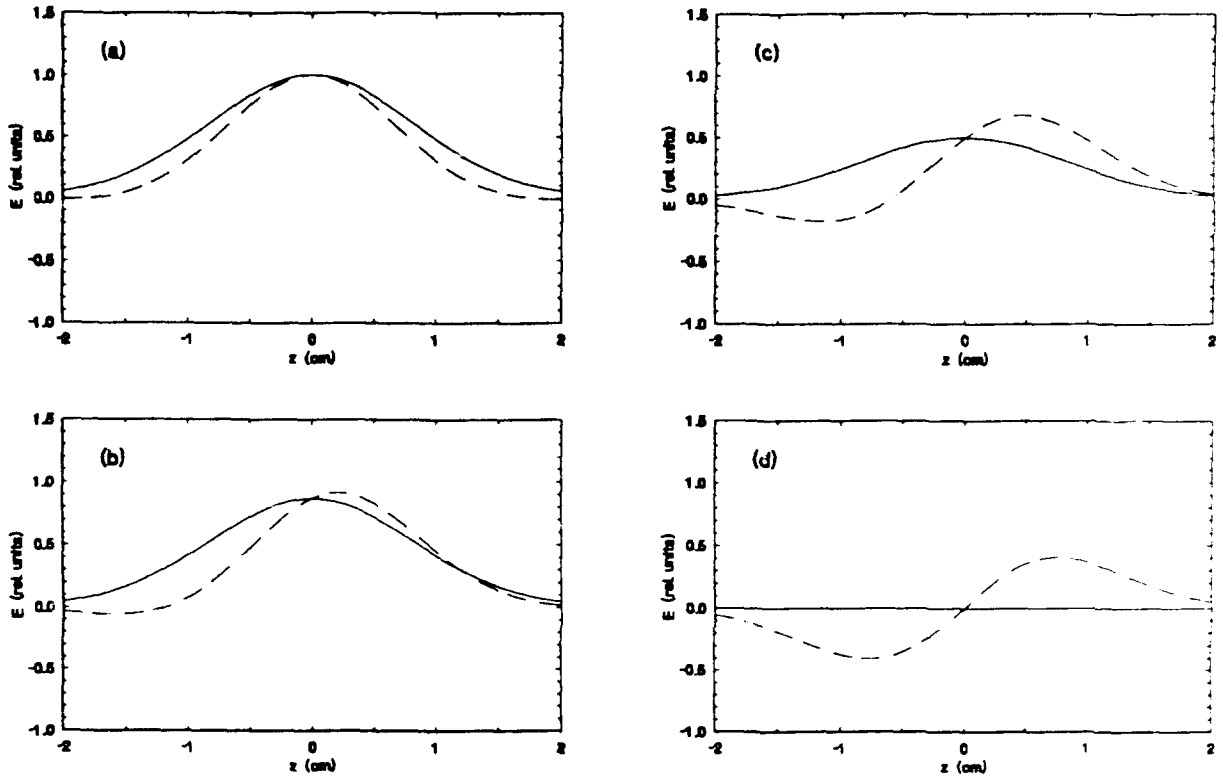


Figure 4: The electric field experienced by an electron in an untilted resonator (solid curve) and a resonator tilted 2° (dashed curve). The positions of the electrons relative to the electric field peak of a single resonator mode is $y = 0$ (a), $\lambda/12$ (b), $\lambda/6$ (c), $\lambda/4$ (d).

by understanding the electric field that each electron experiences as it passes through the resonator. The steady-state electric field of a single mode in the resonator is¹³

$$\mathbf{E}(x, y, z, t) = \hat{\mathbf{x}}E_0 \exp \left[- \left(x^2 + z^2 \right) / w_0^2 \right] \cos \{ k (y - \theta z) \} \cos (\omega t) . \quad (5)$$

This electric field is plotted in Fig. 4 for different y positions in both a tilted ($\theta = 2^\circ$) and an untilted resonator. Two features are important here. First, the electrons in the untilted resonator see simple gaussian profiles with the peak amplitude decreasing to zero as the electrons guiding center moves toward the null of the resonator mode. In the tilted resonator, however, each of the electrons pass through regions of relatively high electric field and thus has the opportunity to interact efficiently with each mode in the resonator. Each electron interacts strongly with all of the resonator modes, making suppression of undesired modes by the main mode relatively effective, increasing the size of the single-mode stability region. The second feature is that the effective interaction length in the tilted resonator is somewhat smaller than in the untilted resonator, and the different electrons in the tilted resonator experience varying amounts of a double peaked electric field. The double peaked electric field is similar to that in a cavity gyrotron operating with an axial mode number of two, and is consistent with the need for the tilted resonator to operate with larger values

of the detuning parameter δ .

III. NUMERICAL RESULTS

The resonator used in the experiments described here was highly overmoded, necessitating the use of a theory that includes the effects of multiple resonator modes. The basic model used in the time-dependent, multimode simulations has been described elsewhere¹⁵ but has been enhanced to better model the actual experiment. These enhancements include the finite rise time of the voltage waveform and its ripple on the 'flat top,' the variation of the longitudinal velocity with position in the resonator due to space charge depression, and the nonuniform magnetic field produced by the magnet used in the experiment.

The rise of the voltage pulse was simulated with a linear increase of the electron energy from 1/2 of the final value up to its flat-top value. The neglect of electron energies less than 1/2 of the final value is justified because they are far from resonance with the final modes in the resonator. The energy rise occurred over a period of 2 μ sec in the simulation, representing the 10-90% rise time of 4 μ sec in the experiment.

The voltage pulse produced by the modulator had a peak-to-peak voltage ripple of $\pm 1.5\%$ during the 'flat top'. The period of the ripple was 2 μ sec. This variation was incorporated directly into the numerical simulations.

The variation of the electron's velocity component parallel to the magnetic field (u_{\parallel}) with position (along the magnetic field axis) in the resonator (ξ) due to space-charge depression is modeled as

$$u_{\parallel} = \left[1 - \left(\frac{\Delta V}{V_0} \right) (\alpha^2 + 1) \cos(\xi\pi/4) \right]^{1/2} \quad (6)$$

where $\Delta V/V_0$ is the voltage depression parameter.

The magnet used in the experiment produced a nonuniform field in the resonator due to the magnet's coils being separated slightly more than in a Helmholtz configuration. This was necessary to maximize the clearance in the cross-bore of the magnet and allow the radiation produced to freely propagate out of the vacuum dewar. The magnetic field in the interaction region was well approximated by assuming a quadratic dependence to the field.

The goal of the numerical simulations was to model the experiment as accurately as possible. Accordingly, the actual voltage and current measured in the experiment were used for the different simulation points. Also, the α values used were based on numerical simulations of the electron gun. Other parameters used in the simulation were also those of the experiment and are listed in Table I.

An example of the time history of the mode amplitudes is shown in Fig. 5. The voltage was 108 kV and the current was 30 A. The final detuning of the zero-mode (e.g., the center mode in the simulation) was $\delta = 4.0$. The α value assumed for the electron beam was 1.3 and the voltage depression parameter $\Delta V/V_0$ was 7%.

The sensitivity of the simulation to the final value of the zero-mode detuning (δ_0) was tested by repeating the calculations with $\delta_0 = 4.2$ and 4.4. Due to the uniform spacing of the modes in the Fabry-Perot resonator it is only necessary to vary δ_0 by amounts less than

Table I: Parameters used in the numerical simulation.

Mirror radius of curvature	38.7 cm
Mirror separation	21.2 cm
Electron beam radius	0.5 cm
Voltage rise time (50-100%)	2 μ sec
Voltage ripple	$\pm 1.5\%$
Resonator output coupling	3.25%
Magnetic field taper	-2%
Resonator tilt angle	2°
Beam voltage	70-110 kV
Beam current	4-65 A
$\Delta V/V_0$	1.5-13.5%
α	1.5-1.2

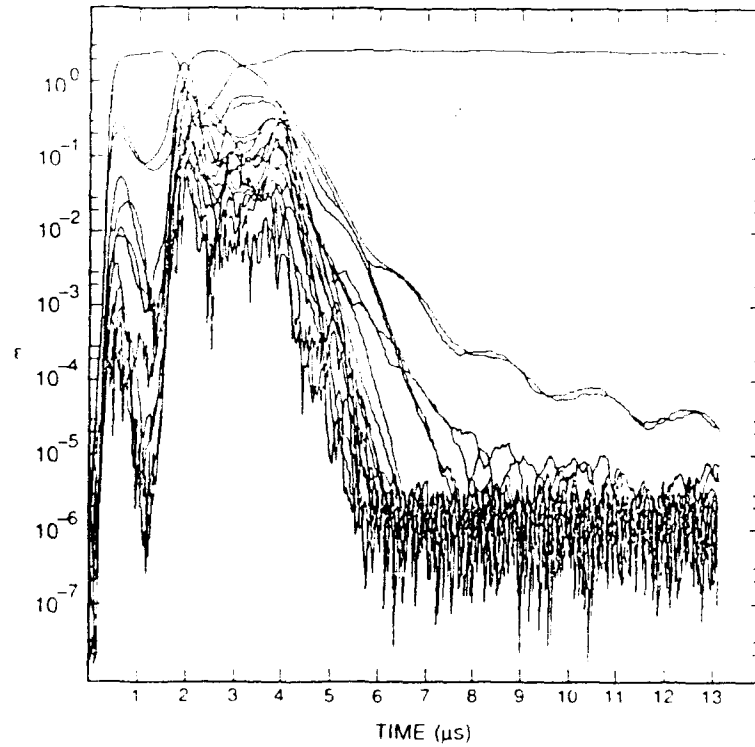


Figure 5: The evolution of the mode amplitudes calculated in the numerical simulation. The current was 30 A and the final detuning of the zero-mode was $\delta_0 = 4.0$.

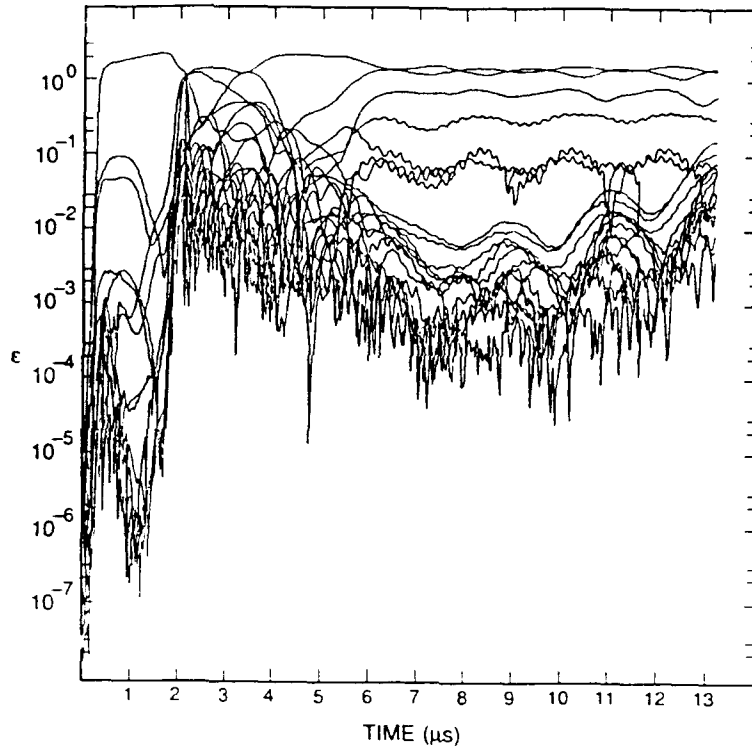


Figure 6: The evolution of the mode amplitudes calculated in the numerical simulation. The parameters are identical to those of Fig. 5 except that $\delta_0 = 4.2$.

$2\pi/T_0$ which is approximately $1/2$ for our experiment.¹⁵ As can be seen from Fig. 6 and Fig. 7, changing the zero-mode detuning has a significant effect on the time evolution of the mode amplitudes. This is due to the fact that the current is such that it passes close to the stability boundary.¹⁵ Therefore, small changes in the detuning could bring the gyrotron to operate in a single mode (if the final state is inside the stable region), or operation could be multimoded (if the final state is outside the stable region). An additional complication is introduced by the $\pm 1.5\%$ voltage ripple, which translates into a detuning variation of 0.4. The average efficiency computed during the flat top of the voltage pulse was 25.8%, 20.3%, and 22.7% for $\delta_0 = 4.0, 4.2, \text{ and } 4.4$ respectively.

Sensitivity of the simulation to the space charge depression parameter $\Delta V/V_0$ was tested at the higher currents. The largest change observed was at a current of 55 A where values of 11% and 16% were used for $\Delta V/V_0$. In this case the average efficiency during the voltage pulse flat top decreased from 22.4% to 20.6% when the space charge depression parameter was increased. Similar variations in this parameter were applied at each current value simulated above 40 A, with the lower value of the parameter being the value predicted by an analytic theory.⁸

IV. DESCRIPTION OF EXPERIMENT

A QOG experiment designed to produce 0.5 MW of rf radiation at a frequency of 120 GHz has been assembled at NRL. A brief description of the experiment is presented here, with the design equations¹⁰ and a more detailed experiment description¹⁶ presented

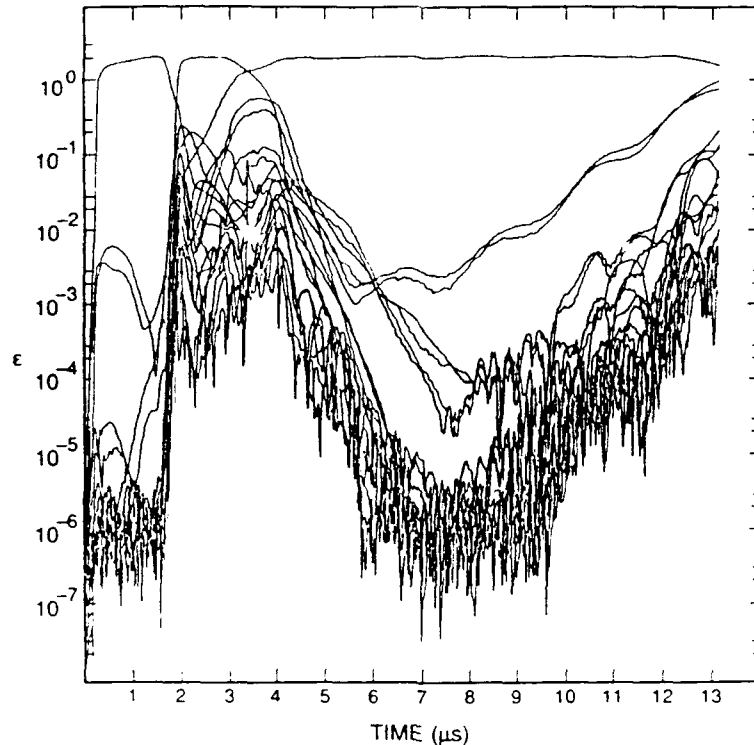


Figure 7: The evolution of the mode amplitudes calculated in the numerical simulation. The parameters are identical to those of Fig. 5 except that $\delta_0 = 4.4$.

elsewhere. A schematic diagram of the experiment is shown in Fig. 8. The gyrating electron beam is generated by a magnetron injection gun located below and in the fringing magnetic field of the superconducting magnet. The beam propagates up through the drift tube, across the open resonator, through the uptaper, and is finally absorbed in the collector, located above the magnet dewar. A low-field trim coil is located just below the collector to prevent the beam electrons from expanding too rapidly and being collected prior to reaching the collector. The microwave fields interact with the electron beam in the open region between the drift tube and the tip of the uptaper. The resonator axis in this experiment was tilted by 2° with respect to the plane perpendicular to the electron beam axis, as indicated in Fig. 9. The microwave power diffracted around each mirror is collected as output and propagated through thin mylar windows out of the vacuum enclosure. Typical parameters of the experiment are given in Table II.

The Varian VUW-8144 electron gun¹⁷ used in this experiment was originally designed for use in the MIT megawatt gyrotron program.¹⁸ Due to the relative insensitivity of the QOG to the electron beam radius, the emitter could be placed in the magnetic field necessary for high perpendicular to parallel velocity ratios (α) in the resonator. Simulation of the beam electrons was accomplished using a standard trajectory-tracing code,¹⁹ which indicated that achievable values of average α ranged from 1.8 with a spread (standard deviation in α) of 13% at low currents to 1.3 with a spread of 23% at 50 A. The simulations indicated that reasonable gun performance could be obtained with the emitter placed in a magnetic field yielding a compression ratio of 24. In this position, the beam in the cavity had a mean

Table II: Typical parameters of the NRL QOG experiment.

Frequency (f)	120 GHz
Electron Energy	112 keV
Electron Current	50 A
Mirror Diameter ($2a$)	4.5 cm
Radius of Curvature (R_c)	38.7 cm
Mirror Separation (d)	21.2 cm
Longitudinal Mode Spacing ($\Delta f/f$)	0.59%
Radiation Waist Radius (w_o)	1.17 cm
Electron Beam Radius	5.6 mm
Electron Beam Thickness	0.5 mm
Normalized Interaction Length (μ)	12
Output Coupling (T , round trip)	3.1%
Diffraction Quality Factor (Q_d)	34,850
Ohmic Quality Factor (Q_o)	438,000
Total Quality Factor (Q)	32,280
Normalized Electric Field (F)	0.13
Output Power	430 kW
Peak Ohmic Heating Density	5.4 kW/cm ²
Total Ohmic Power (per mirror)	15.6 kW
Number of Interacting Modes	~ 7

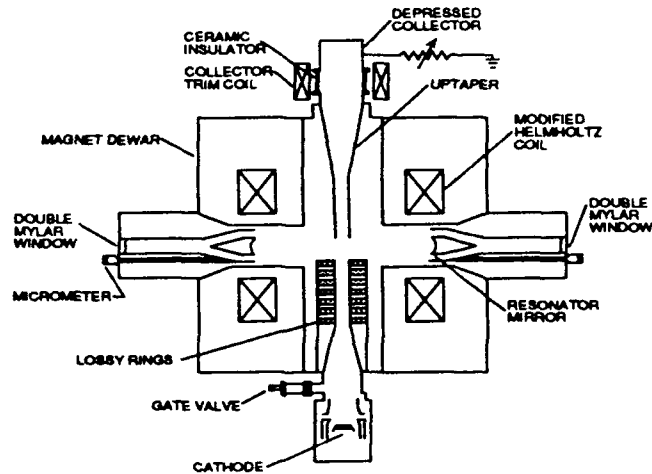


Figure 8: Schematic diagram of the NRL QOG experiment.

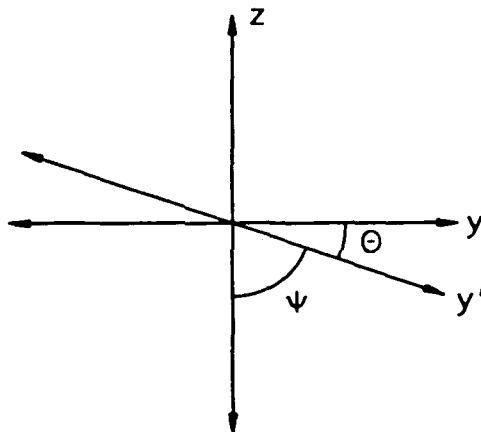


Figure 9: Orientation of the resonator and electron beam axes.

radius of 0.56 cm and a thickness of 0.05 cm.

The electron gun has been operated at voltages up to 110 kV and currents up to 65 A, driven by a modulator producing 13 μsec voltage pulses. The 10–90% rise time and the 90–10% fall times were approximately 4 μsec each and there was approximately $\pm 1.8\%$ ripple on the voltage flat top. With the magnetic field and cathode voltage fixed, the beam α could be varied by changing the voltage applied to the intermediate anode of the gun. The ratio of intermediate anode voltage to cathode voltage ($V_{\text{int}}/V_{\text{cat}}$) was set by a voltage divider and varied in the experiment from 0.63 to 0.68. At low ratios, corresponding to large electric fields at the cathode, gun simulations predicted total reflection of the electron beam. Experimentally, the beam did propagate, however, the current diagnostics for the collector, drift tube, uptaper, and intermediate anode became very noisy. To understand this anomaly, one must understand the differences between the gun simulations and the experiment. The simulations assume a steady state, with the gun voltages already applied

and the current at the final value. In the experiment, the electron gun voltages are pulsed on, with a rise time of approximately 4 μ sec. The electron beam current rise time is somewhat faster, approximately 2 μ sec, due to the emission being temperature limited. As the electron gun voltage is pulsed on, both the intermediate anode and the cathode voltage rise with their ratio remaining constant. At lower voltages, the current is predicted by the simulations to propagate, reflecting only when the voltage rises above a threshold value. It is possible that some of the electrons are reflected back toward the electron gun during the rise of the voltage pulse, creating a charge density great enough to shield out some portion of the intermediate anode voltage at the cathode. If the electric field at the cathode is depressed enough, the transverse velocity will be reduced ($v_{\perp} \propto E_{\text{cathode}}/B_{\text{cathode}}$) to the point that reflection does not occur and the electron beam will again be able to propagate to the resonator. The large noise associated with this phenomena may be due to the space charge cloud formed by reflexing electrons and associated instabilities.

V. EXPERIMENTAL RESULTS

A large volume of data was collected over a period of several months; the most significant of which is presented here. The magnetic field was set at 4.7 T at the center of the resonator and data was obtained for tapers of -2%, 0%, and +2%. The best results were obtained with a taper of -2%, i.e., the magnetic field tapered from 1% greater 2.4 cm closer to the electron gun to a value 1% lower 2.4 cm closer to the collector. For each value of current, the cathode voltage was varied, producing data at several different gun voltages. Typically, for a given intermediate anode voltage divider setting and current, there is a single electron gun voltage which produced the highest efficiency and this is the data point reported here. Data of this type was collected for a single resonator tilted at an angle of 2° and compared to similar data taken with the same resonator untilted (tilt angle of 0°).

The output power of the tilted resonator is plotted as a function of electron beam current in Fig. 10. The magnetic field taper for this data was -2%. The output power reached a level of 597 kW, a record for quasioptical gyrotrons, at a gun voltage of 110 kV and a current of 65 A. The output power was calculated by dividing the average power measured by a modified laser calorimeter by the voltage flat-top pulse width and the repetition rate. The calorimeter power was corrected for the finite absorptivity (95%) of the calorimeter, but no corrections for window, waveguide, or other losses were included. The efficiency of this data was calculated by dividing the output power by the gun voltage and the current passing through the resonator, and is plotted in Fig. 11. The peak efficiency of 12.3% was reached at a voltage of 87 kV and a current of 14 A, and the efficiency dropped to nearly 8% at the highest output powers. As the current was increased, the gun voltage for optimum efficiency also increased, as shown in Fig. 12. Part of this increase in voltage is necessary to offset the increased voltage depression of the electron beam due to increased space charge as the current is raised.

By decreasing the voltage slightly from its optimum the resonator could be made to operate in a single mode; however, the interaction efficiency was somewhat reduced. The power and efficiency of operation in a single mode is shown in Fig. 13. Experimentally, we define single-mode operation as operation with all modes at least 10 dB lower in power

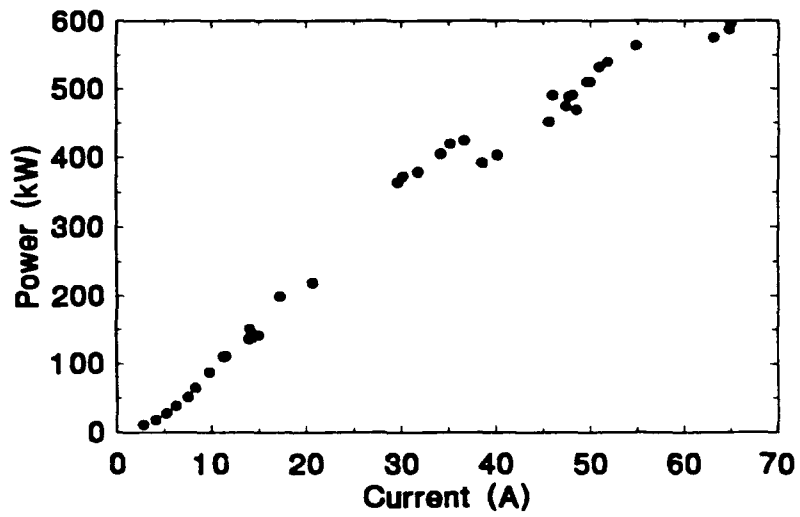


Figure 10: Output power as a function of electron beam current in the NRL quasioptical gyrotron experiment with the resonator tilted 2° .

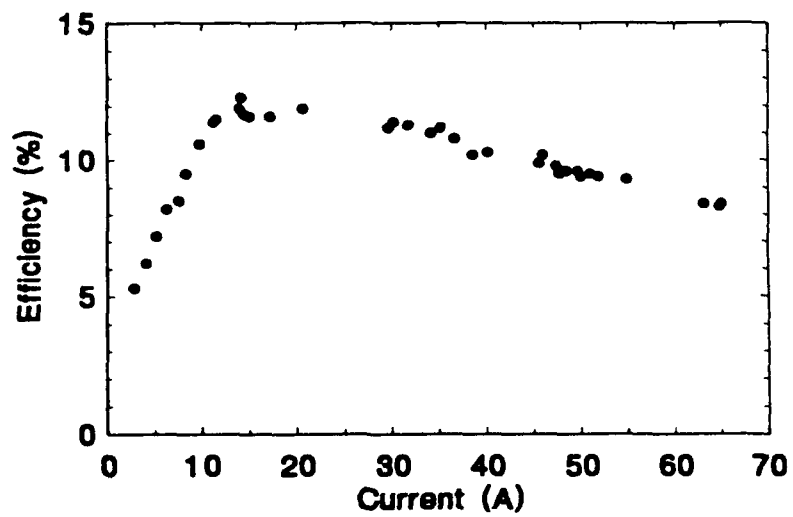


Figure 11: Output efficiency as a function of current for the data shown in Fig. 10.

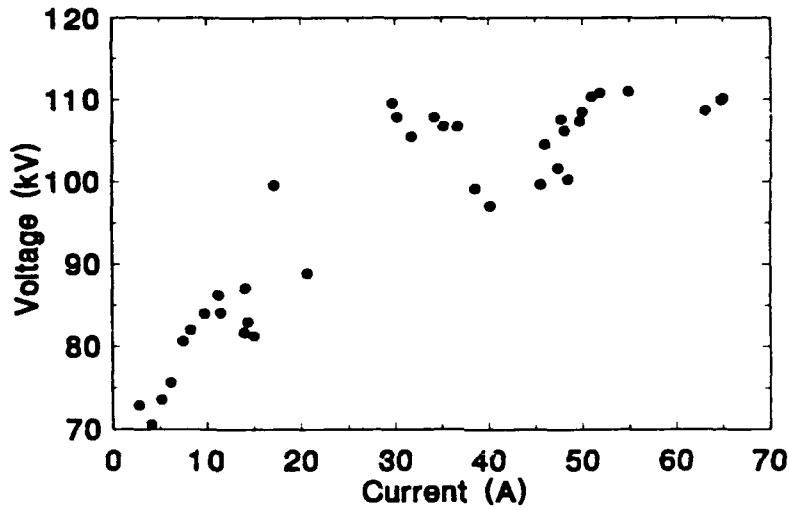


Figure 12: Electron gun cathode voltage as a function of current for the data shown in Fig. 10.

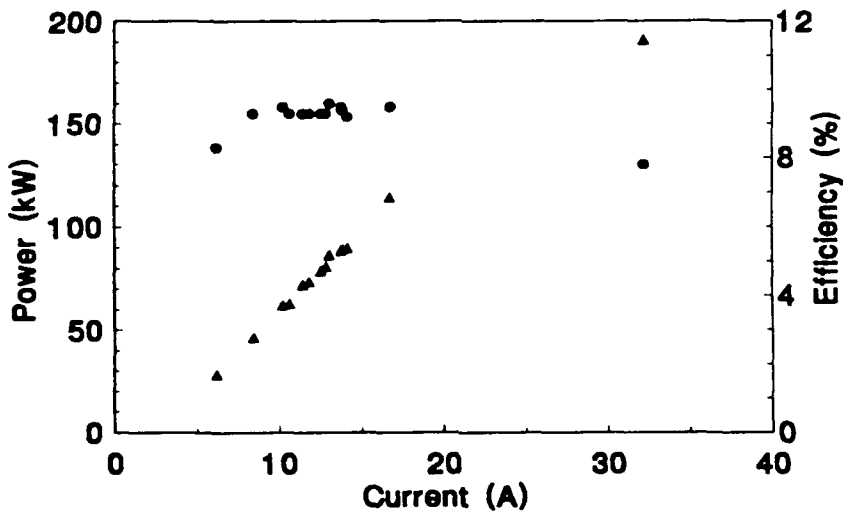


Figure 13: Power (triangles) and efficiency (circles) as a function of electron beam current of the QOG operating in a single mode.

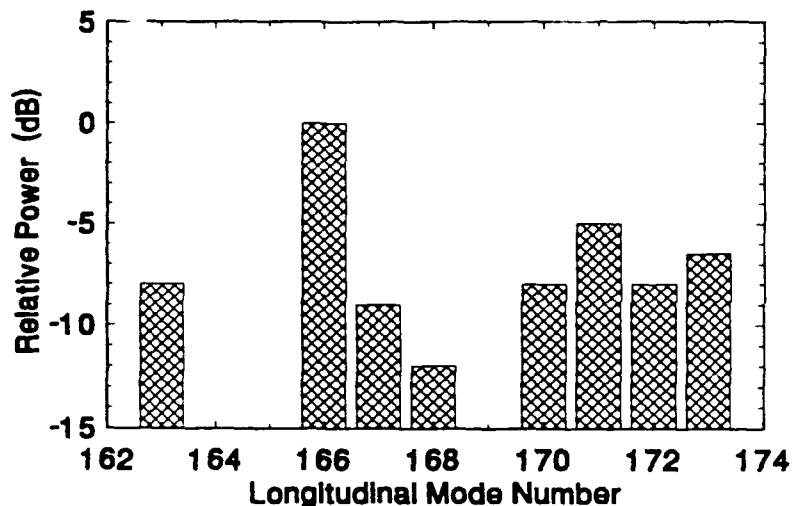


Figure 14: Frequency spectrum of the QOG output during operation at 500 kW. The frequencies have been identified by their longitudinal mode number in the resonator.

than the main mode. The data at 32 A in Fig. 13 indicate a data point where the second most powerful mode is only 8–10 dB lower in power than the principal mode. Some data was taken between 20 and 30 A, but single-mode operation was not obtained, possibly due to difficulties in tuning the modulator to produce a flat, low-ripple voltage waveform. The mode spectrum does not become excessively dense as the output power is increased, as can be seen in Fig. 14. In this case, the output power was 500 kW and the second most powerful mode is 5 dB less powerful than the main mode.

VI. DISCUSSION

The efficiency of operation of the tilted and the untilted resonators are compared in Fig. 15. As can be seen, there is a small difference at low currents, but from the peak of the efficiency up to the maximum current, there is no discernible difference between the tilted and untilted resonator performance. Theoretically, the peak efficiency was not expected to rise significantly when the resonator was tilted, but the current at which the peak efficiency occurred was expected to rise approximately 10%. This small rise may actually have occurred but been beyond the resolution of the data plotted. However, the output mode spectrum of the tilted resonator was expected to be single moded to much higher currents, and the peak efficiency was expected to be in the stable, single-mode operating region.

As can be seen in Fig. 16, the efficiency of single-mode operation was somewhat lower than that of multimode operation for the tilted resonator. This figure should be compared to experimental results of single- and multimode operation of an otherwise identical, but untilted, resonator. Unfortunately, during the operation of the untilted resonator experiment, the frequency diagnostics were unavailable. A somewhat less valid comparison can be

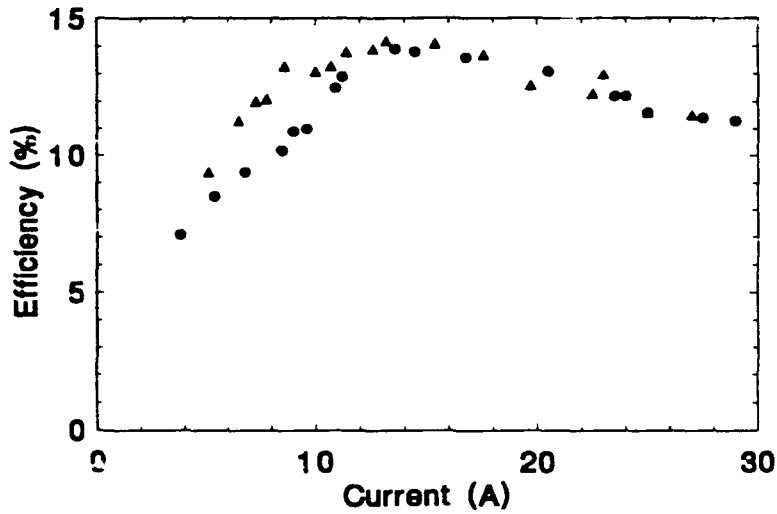


Figure 15: Efficiency as a function of electron beam current with the resonator tilted 2° (triangles) and the resonator untilted (circles).

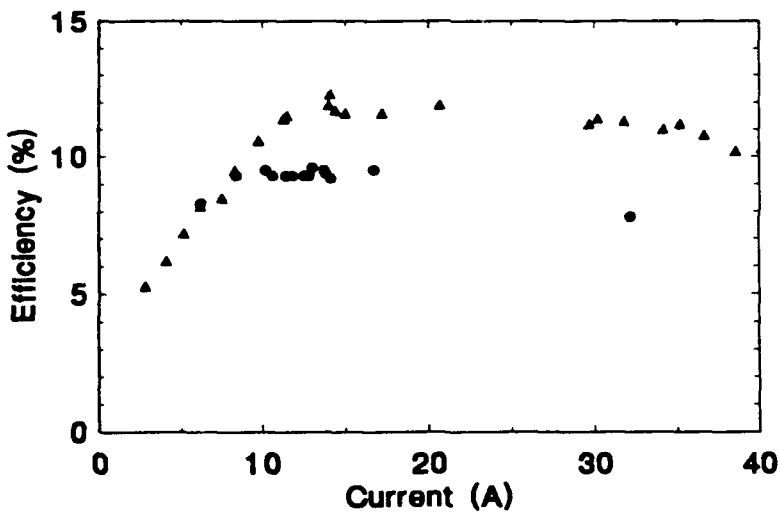


Figure 16: The experimental efficiency for single-mode (circles) and multimode (triangles) operation with a tilted resonator as a function of electron beam current.

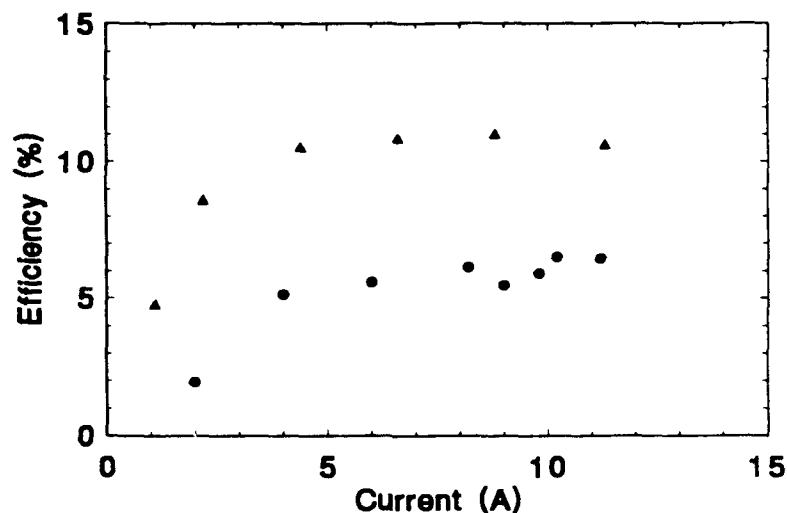


Figure 17: The experimental efficiency for single-mode (circles) and multimode (triangles) operation of an earlier QOG experiment^{8, 20} with an untilted resonator as a function of electron beam current.

made with data taken during an earlier experiment^{8, 20} that utilized a less powerful electron gun and a resonator with correspondingly lower output coupling. The separation of the resonator mirrors was approximately the same in the both experiments. The efficiencies of single- and multimode operation of the earlier (untilted resonator) experiment are shown in Fig. 17. It is evident from Figs. 16 and 17 that the tilting of the resonator was successful in bringing the single-mode efficiency closer to the efficiency of multimode operation, but that the multimode regime results in the highest efficiency for both the tilted and the untilted resonators.

A possible interpretation of these experimental results is the following. An untilted resonator has many electrons passing through (or near) nulls of the standing electric field in the resonator. These electrons do not contribute to the beam-wave interaction and hence, their presence lowers the operating efficiency. Anything which makes all of the electrons interact strongly with the resonator fields will raise the efficiency. A multimode spectrum in the resonator will have this effect; each electron will see nearly the same time-averaged electric field. This is a possible explanation of the fact that the single-mode efficiency is so much lower than the multimode efficiency in the earlier experiment.^{8, 20} Tilting the resonator axis will have much the same effect on the efficiency as multimode operation in that it allows each electron to interact with a large amplitude electric field in the resonator, even during single-mode operation. Additionally operating in the multimode regime with a tilted resonator may not affect the efficiency much, as is evidenced by the fact that the single-mode and multimode efficiencies measured in the tilted resonator experiment are much closer in value than in the untilted resonator experiment. Thus, tilting the resonator axis is successful in bringing the single-mode efficiency nearly up to the multimode efficiency level. However, it is not successful in raising either the single-mode or the multimode efficiency up to the theoretically predicted value.

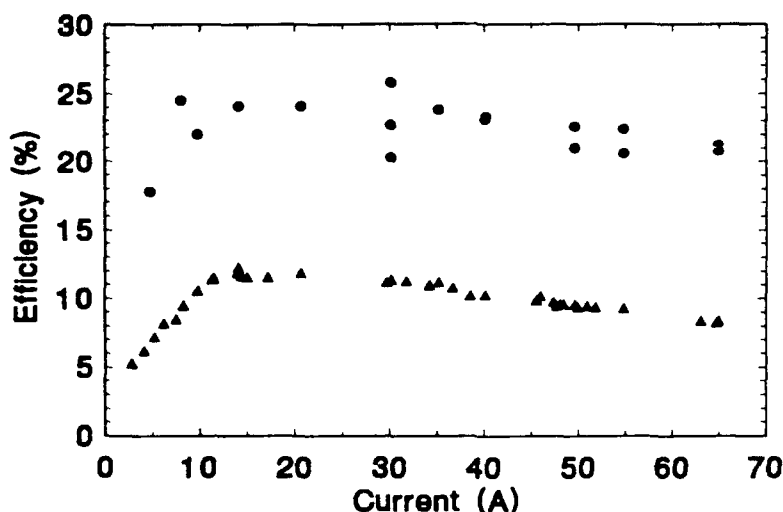


Figure 18: The experimental efficiency (triangles) and the efficiency calculated in the numerical simulations (circles) as a function of electron beam current. The variation of the efficiency calculated in the simulations at 30 A is due to using different values of the zero-mode detuning parameter δ_0 . The different efficiencies produced by the simulations at higher currents were due to using different values of the space charge depression parameter $\Delta V/V_0$.

As many of the experimental features were included in the numerical simulations as possible. Features not included were the spread in the electron beam α and the full rise and fall of the voltage pulse. As noted above, the first half of the voltage rise is not expected to be important, and it was not feasible to include a spread in beam α due to the added length of the computation. The effect of beam α spread was examined separately with a single-mode computation²¹ where it was found that a RMS spread of $\pm 35\%$ about a mean α of 1.93 did not significantly affect the output efficiency. The spread in beam α in the experiment is expected to be somewhat less than the value of 35% used in the simulation. The efficiency in the simulation was calculated by averaging the instantaneous efficiency over the time of the flat-top of the voltage pulse and is plotted with the experimental efficiency in Fig. 18. The three theoretical points at 30 A were obtained by varying the zero-mode detuning (δ_0) as noted above. The multiple points at single current values above 40 A were obtained by varying the space charge depression parameter ($\Delta V/V_0$). For example, at 50 A the values of 11% and 14% were used for $\Delta V/V_0$. Similar values were used for the other points, with the lower value predicted by an analytic model⁸ using the experimental parameters. Higher values of the space charge depression parameter resulted in lower calculated efficiencies in all cases.

Several possible explanations exist for the discrepancy between the experimental results and the multimode calculations. One possibility is that the resonator modes are higher-order transverse modes, for instance the $TEM_{0,1}$ mode. Although this mode has higher diffraction losses than the fundamental $TEM_{0,0}$ mode, it has better coupling to the electron

beam since its fields are more concentrated along the path of the beam. Initial stability calculations indicate that when both fundamental and higher order modes are present, the $TEM_{0,1}$ mode is suppressed by the fundamental $TEM_{0,0}$ mode.²¹ A second possibility is that some second harmonic radiation grows in the resonator and affects the interaction between the electron beam and the fundamental mode. Second harmonic radiation has been observed in QOG experiments performed elsewhere,²² but was not seen in the experiments described here despite an effort to measure it. Another possibility is that the quality of the electron beam is much worse than predicted by the electron gun design codes used. There is some evidence of this in cavity gyrotrons, where beam diagnostic experiments are being performed on similar electron guns.²³ Finally, it is possible that the electron beam is driving oscillations in the beam transport system before reaching the resonator, bunching the beam and adding a large energy spread.²¹ Attempts have been made to measure radiation leaking out of the system through the bottom of the electron gun, but no power has been observed.

These questions will be answered in an experiment currently being designed.^{24, 25} A prebunching resonator will be added to the system to form a quasioptical gyrokystron. The prebunching resonator will be inserted into the current electron beam transport system, essentially adding a diagnostic port for observation of unwanted oscillations. Additional information about the quality of the beam will be gained by measuring the threshold current for oscillation in the prebunching resonator. Capacitive probes will also be added to the beam transport system to measure the average α value of the electron beam. A second modification of the experiment will increase the mirror separation to approximately 95 cm. This will place the resonator mirrors at the vacuum windows, allowing the radiation to propagate freely out of the vacuum (e.g. without reflection) so that the radiation pattern can be directly measured. This measurement should allow one to determine the mode operating in the resonator. The larger mirror separation will also allow the insertion into the resonator of a thin dielectric to act as a beam splitter and reflect a small amount of the radiation out of the vacuum system, enabling the radiation pattern within the resonator to be measured. In particular, any sizable amount of second harmonic radiation should be observable.

VII. CONCLUSIONS

A QOG experiment has been performed with a resonator tilted by 2° relative to the plane perpendicular to the magnetic field in the resonator. The efficiency of operation of the tilted and untilted resonators was slightly different at currents below that for optimum efficiency, but were virtually identical at currents above the peak efficiency. The tilted resonator could be operated in a single mode over a relatively large range of currents, but only by lowering the electron gun voltage and operating at a reduced efficiency. However, this reduced efficiency is much closer to the optimum multimode efficiency than the single-mode efficiency of an untilted resonator is to its corresponding multimode efficiency.

The tilted resonator produced a maximum power of 597 kW at an efficiency of 8.3% and a frequency of 120 GHz. The peak efficiency of 12.3% occurred at an output power of 150 kW. These efficiencies are a factor of 2-3 lower than those predicted by multimode simulations including the experimental realities of finite voltage rise time, voltage ripple,

variation of the longitudinal velocity of the electrons due to space charge depression, and the nonuniform magnetic field. Possible explanations of this difference include much larger electron beam velocity spreads than predicted by the standard design tools, large energy spread due to oscillations in the beam transport system, operation of a higher-order transverse mode in the resonator, and operation of the second harmonic in the resonator. An experiment designed to address each of these problems is currently being designed.

ACKNOWLEDGEMENTS

We thank Drs. Steven Gold and Robert McCowan for their many helpful discussions. This work was supported by the Office of Fusion Energy of the U. S. Department of Energy and by the Office of Naval Research.

References

- ¹ G. H. Neilson and THE CIT TEAM, "Physics design of the compact ignition tokamak," *Bull. Am. Phys. Soc.*, vol. 35, no. 9, p. 2105, 1990.
- ² V. S. Mukhovatov for ITER Team, "ITER operation and diagnostics," *Rev. Sci. Instrum.*, vol. 61, no. 10, p. 3241, 1990.
- ³ K. Felch, R. Bier, L. J. Craig, H. Huey, L. Ives, H. Jory, N. Lopez, and S. Spang, "CW operation of a 140 GHz gyrotron," *Int. J. Elec.*, vol. 61, p. 701, 1986.
- ⁴ K. Felch. private communication.
- ⁵ K. E. Kreischer. private communication.
- ⁶ P. Sprangle, J. Vomvoridis, and W. M. Manheimer, "A classical electron cyclotron quasioptical maser," *Appl. Phys. Lett.*, vol. 38, no. 5, p. 310, 1981.
- ⁷ A. Bondeson, W. M. Manheimer, and E. Ott, *Infrared and Millimeter Waves*, ch. 7. Vol. 9, Academic Press, 1983.
- ⁸ A. W. Fliflet, T. A. Hargreaves, W. M. Manheimer, R. P. Fischer, and M. L. Barsanti, "Operating characteristics of a continuous-wave-relevant quasioptical gyrotron with variable mirror separation," *Phys. Fluids B*, vol. 2, no. 5, p. 1046, 1990.
- ⁹ T. A. Hargreaves, A. W. Fliflet, R. P. Fischer, and M. L. Barsanti, "Depressed collector performance on a quasioptical gyrotron," *submitted to Phys. Fluids B*, vol. 1, p. 1, 1991.
- ¹⁰ A. W. Fliflet, T. A. Hargreaves, R. P. Fischer, W. M. Manheimer, and P. Sprangle, "Review of quasioptical gyrotron development," *J. Fusion Energy*, vol. 9, p. 31, 1990.
- ¹¹ J. P. Hogge, H. Cao, W. Kasperek, T. M. Tran, and M. Q. Tran, "Output coupling of a quasioptical fabry-perot resonator by means of a diffractive grating in the mm wave range," in *Fifteenth International Conference on Infrared and Millimeter Waves*. (R. J. Temkin, ed.), p. 535, SPIE, Bellingham, WA, 1990.
- ¹² A. G. Luchinin and G. S. Nusinovich, "An analytical theory for comparing the efficiency of gyrotrons with various electrodynamic systems," *Int. J. Elec.*, vol. 57, no. 6, p. 827, 1984.
- ¹³ T. M. Antonsen, Jr., B. Levush, and W. M. Manheimer, "Stable single mode operation of a quasioptical gyrotron," *Phys. Fluids B*, vol. 2, no. 2, p. 419, 1990.
- ¹⁴ B. G. Danly and R. J. Temkin, "Generalized nonlinear harmonic gyrotron theory," *Phys. Fluids*, vol. 29, no. 2, p. 561, 1986.
- ¹⁵ B. Levush and T. M. Antonsen, Jr., "Mode competition and control in high-power gyrotron oscillators," *IEEE Trans. Plasma Sci.*, vol. 18, p. 260, June 1990.

- ¹⁶ A. W. Fliflet, T. A. Hargreaves, W. M. Manheimer, R. P. Fischer, and M. L. Barsanti, "Initial operation of a high-power quasioptical gyrotron," *IEEE Trans. Plasma Sci.*, vol. 18, p. 306, 1990.
- ¹⁷ H. Huey, N. Lopez, R. Garcia, and K. E. Kreischer, "A magnetron injection gun for the MIT megawatt gyrotron," in *Tenth International Conference on Infrared and Millimeter Waves*, (R. J. Temkin, ed.), p. 223, IEEE, New York, NY, 1985.
- ¹⁸ K. E. Kreischer and R. J. Temkin, "Single-mode operation of a high-power, step-tunable gyrotron," *Phys. Rev. Lett.*, vol. 59, no. 5, p. 547, 1987.
- ¹⁹ W. B. Herrmannsfeldt, "Electron trajectory program," SLAC Report 226, Stanford Linear Accelerator Center, November 1979.
- ²⁰ A. W. Fliflet, T. A. Hargreaves, W. M. Manheimer, R. P. Fischer, and M. L. Barsanti, "Operation of a quasioptical gyrotron with variable mirror separation," *Phys. Rev. Lett.*, vol. 62, no. 23, p. 2664, 1989.
- ²¹ G. Saraph, G. I. Lin, T. M. Antonsen, Jr., and B. Levush, "Regions of single mode operation in high power gyrotron oscillator," in *Fifteenth International Conference on Infrared and Millimeter Waves*, (R. J. Temkin, ed.), p. 511, SPIE, Bellingham, WA, 1990.
- ²² S. Alberti, M. Q. Tran, J. P. Hogge, T. M. Tran, A. Bondeson, P. Muggli, A. Perrenoud, B. Jödicke, and H. G. Mathews, "Experimental measurements on a 100 GHz frequency tunable quasioptical gyrotron," *Phys. Fluids B*, vol. 2, no. 7, p. 1654, 1990.
- ²³ W. C. Guss, T. L. Grimm, K. E. Kreischer, and R. J. Temkin, "Beam diagnostic measurements in a 140 GHz megawatt gyrotron," in *Fifteenth International Conference on Infrared and Millimeter Waves*, (R. J. Temkin, ed.), p. 416, SPIE, Bellingham, WA, 1990.
- ²⁴ W. M. Manheimer, B. Levush, and T. M. Antonsen, Jr., "Equilibrium and stability of free-running, phase-locked, and mode-locked quasioptical gyrotrons," *IEEE Trans. Plasma Sci.*, vol. 18, p. 350, 1990.
- ²⁵ R. P. Fischer and W. M. Manheimer, "A two-cavity quasioptical gyrotron," in *Fifteenth International Conference on Infrared and Millimeter Waves*, (R. J. Temkin, ed.), p. 505, SPIE, Bellingham, WA, 1990.